Immunity
Article

A Molecular Basis for the Control of Preimmune Escape Variants by HIV-Specific CD8+ T Cells

Kristin Ladell,[1,11] Masao Hashimoto,[2,11] Maria Candela Iglesias,[3,11] Pascal G. Wilmann,[4,11] James E. McLaren,[1] Stéphanie Gras,[4] Takayuki Chikata,[2] Nozomi Kuse,[2] Solène Fastenackels,[3] Emma Gostick,[1] John S. Bridgeman,[1] Vanessa Venturi,[5] Zaïna Aït Arkoub,[6] Henri Agut,[6] David J. van Bockel,[7] Jorge R. Almeida,[3,8] Daniel C. Douek,[8] Laurence Meyer,[9] Alain Venet,[9] Masafumi Takiguchi,[2,12] Jamie Rossjohn,[1,4,12] David A. Price,[1,8,12] and Victor Appay[3,10,12,*]

[1]Institute of Infection and Immunity, Cardiff University School of Medicine, Heath Park, Cardiff CF14 4XN, Wales, UK
[2]Center for AIDS Research, Kumamoto University, 2-2-1 Honjo, Kumamoto 860-0811, Japan
[3]INSERM UMR S 945, Infections and Immunity, Université Pierre et Marie Curie-Paris6, Hôpital Pitié-Salpêtrière, 75013 Paris, France
[4]Department of Biochemistry and Molecular Biology, School of Biomedical Sciences, Monash University, Victoria 3800, Australia
[5]Computational Biology Group, Centre for Vascular Research, University of New South Wales, Kensington, Sydney, NSW 2052, Australia
[6]Virology Laboratory, ER1 DETIV UPMC, Université Pierre et Marie Curie-Paris6, Hôpital Pitié-Salpêtrière, 75013 Paris, France
[7]St Vincent's Centre for Applied Medical Research and University of New South Wales, Darlinghurst, Sydney, NSW 2010, Australia
[8]Human Immunology Section, Vaccine Research Center, National Institute of Allergy and Infectious Diseases, National Institutes of Health, Bethesda, MD 20892, USA
[9]INSERM, Université Paris-Sud, Hôpital du Kremlin-Bicêtre, 94275 Le Kremlin-Bicêtre, France
[10]AP-HP, Groupe Hospitalier Pitié-Salpêtrière, Laboratoire d'Immunologie Cellulaire et Tissulaire, 75013 Paris, France
[11]These authors contributed equally to this work
[12]These authors contributed equally to this work
*Correspondence: victor.appay@upmc.fr
http://dx.doi.org/10.1016/j.immuni.2012.11.021

SUMMARY

The capacity of the immune system to adapt to rapidly evolving viruses is a primary feature of effective immunity, yet its molecular basis is unclear. Here, we investigated protective HIV-1-specific CD8+ T cell responses directed against the immunodominant p24 Gag-derived epitope KK10 ($KRWIILGLNK_{263-272}$) presented by human leukocyte antigen (HLA)-B*2705. We found that cross-reactive CD8+ T cell clonotypes were mobilized to counter the rapid emergence of HIV-1 variants that can directly affect T cell receptor (TCR) recognition. These newly recruited clonotypes expressed TCRs that engaged wild-type and mutant KK10 antigens with similar affinities and almost identical docking modes, thereby accounting for their antiviral efficacy in HLA-B*2705+ individuals. A protective CD8+ T cell repertoire therefore encompasses the capacity to control TCR-accessible mutations, ultimately driving the development of more complex viral escape variants that disrupt antigen presentation.

INTRODUCTION

Adaptive CD8+ T cell immunity is critical for protection against viruses and other intracellular pathogens. At the molecular level, this host-pathogen conflict centers on T cell receptor (TCR) engagement of major histocompatibility complex class I (MHC-I) molecules bearing peptide fragments derived from the intracellular invader. The αβ TCR repertoire encompasses a phenomenal level of diversity, which is generated by somatic recombination of variable (V), diversity (D), and joining (J) gene segments, junctional modifications, and differential pairing of α and β chains. Theoretically, between 10^{15} and 10^{20} different TCRs can be generated by this process (Davis and Bjorkman, 1988; Lieber, 1991). However, because of size constraints and thymic selection, each individual harbors a repertoire estimated to contain around 2.5×10^7 TCRs (Arstila et al., 1999). The diversity of the peripheral TCR repertoire has profound implications for effective immune coverage (Nikolich-Zugich et al., 2004).

Rapidly evolving pathogens capable of intrahost evolution during the course of infection must contest with the array of TCRs available for deployment. This sets the stage for a "molecular arms race" between the pathogen and the host. Immune escape by mutation of targeted CD8+ T cell epitopes is a cardinal feature of HIV-1 infection and represents a key obstacle to the successful development of an AIDS vaccine (Goulder and Watkins, 2004). Indeed, the intense antiviral pressure exerted by CD8+ T cell responses drives the rapid selection of escape mutations from the earliest stages of infection (Goonetilleke et al., 2009). Eventually, the frequency of such mutations correlates with the prevalence of the restricting human leukocyte antigen (HLA) class I allele across the population as a whole (Dong et al., 2011; Kawashima et al., 2009; Moore et al., 2002). Nonetheless, certain HLA class I alleles, including HLA-B*27, can confer relative protection from disease progression (Kaslow et al., 1996). In HLA-B*27+ individuals infected with HIV-1 clade B,

the immunodominant KK10 epitope ($KRWIILGLNK_{263-272}$) in p24 Gag is almost invariably targeted by $CD8^+$ T cells (Altfeld et al., 2006; Scherer et al., 2004). These KK10-specific $CD8^+$ T cells unleash potent effector functions (Almeida et al., 2007; Berger et al., 2011), and the conservation of this response is thought to account for the benefits conferred by HLA-B*27 expression.

A number of mutations in the KK10 epitope have been reported in HIV-1-infected patients. The commonly observed Leu268Met mutation was initially considered to be a compensatory change required for the later appearance of the Arg264Lys mutation, which is associated with increased viral loads and clinical progression (Ammaranond et al., 2011; Feeney et al., 2004; Goulder et al., 1997; Kelleher et al., 2001). However, we recently showed that the Leu268Met mutation enables HIV-1 to evade recognition by highly effective $CD8^+$ T cells, including clonotypes defined by the expression of public TRBV4-3 TRBJ1-3 TCRs, which can be shared between individuals responding to the KK10 epitope (Iglesias et al., 2011). Nonetheless, control of viral replication is usually preserved despite this mutation. In HIV-1-infected patients presenting primarily a Leu268Met virus, the KK10-specific $CD8^+$ T cell response seems to be more reactive against the Leu268Met variant compared to the wild-type (WT) epitope; the converse applies in patients presenting a predominant WT virus (Iglesias et al., 2011; Lichterfeld et al., 2007; Streeck et al., 2008). These observations suggest that the immune response can adapt to mutations within the KK10 peptide that remain accessible to the TCR repertoire. However, the precise mechanism responsible for the maintenance of immune control in this situation remains unclear. Here, we show that the immune system can counter the emergence of Leu268Met variants through the mobilization of newly generated cross-reactive KK10-specific $CD8^+$ T cells, in particular those bearing TRBV6-5 TRBJ1-1 TCRs. These clonotypes were able to control both WT and Leu268Met viruses and retained potent suppressive capacity unless the virus succeeded in acquiring mutations, such as Arg264Lys, that negatively impact epitope presentation.

RESULTS

Emergence of Cross-Reactive WT and Leu268Met KK10-Specific $CD8^+$ T Cells during Primary HIV-1 Infection

To understand how KK10-specific $CD8^+$ T cell populations adjust to the early emergence of the Leu268Met mutant and maintain control of viral replication, we examined the fine specificity of responses to this epitope in HLA-B*2705$^+$ patients with primary HIV-1 infection. For this purpose, WT, Leu268Met, or dually reactive KK10-specific $CD8^+$ T cells were identified directly ex vivo by flow cytometry with fluorescent HLA-B*2705-peptide tetramers (Figure 1A). During early infection (i.e., within 3 months of viral transmission), robust $CD8^+$ T cell responses against WT, but not Leu268Met, KK10 could be detected in three patients (Figures 1A and 1B). These $CD8^+$ T cell populations engaged WT KK10 antigen (Ag) with high avidity, as revealed by staining with the corresponding CD8-null tetramer. Previous studies have shown that this physical parameter correlates with potent HIV-suppressive capacity (Almeida et al., 2007, 2009; Berger et al., 2011). Subsequently, we observed $CD8^+$ T cell expansions with reactivity against the Leu268Met variant (Figures 1A and 1B). These distinct populations exhibited high avidities for the cognate Ag in two patients (PrInf A and B) with stable control of viral replication in the absence of antiretroviral therapy. In contrast, lower-avidity Leu268Met KK10-specific $CD8^+$ T cells were present in patient PrInf C, who initiated antiretroviral therapy 18 months after infection as a result of progressively increasing viral loads (Figure 1C).

Extensive viral sequencing, from both plasma and peripheral blood mononuclear cells, was conducted to inform the observed patterns of KK10 reactivity (Figure 1C and Table S1 available online). In PrInf C, expansion of the Leu268Met KK10-specific $CD8^+$ T cell population coincided with the emergence of detectable Leu268Met variant virus at month 18. Indeed, the Leu268Met sequence was dominant at the cell-associated DNA level, indicating that the corresponding variant virus was poorly controlled in this patient. In patients PrInf A and B, however, the high-avidity Leu268Met KK10-specific $CD8^+$ T cell populations expanded without evidence of the Leu268Met mutation. Indeed, the Leu268Met sequence was detected in the cell-associated DNA from PrInf A only at a very late time point, after the initiation of antiretroviral therapy. Collectively, these data indicate that the immune system can generate high-avidity cross-reactive WT and Leu268Met KK10-specific $CD8^+$ T cells soon after primary HIV-1 infection, even with frequencies of Leu268Met variant virus that lie below the limit of detection with conventional sequencing methodologies.

High-Avidity WT and Leu268Met KK10-Specific $CD8^+$ T Cells Incorporate TRBV6-5 TRBJ1-1 Motif-Bearing TCRs

To characterize the molecular basis for WT and Leu268Met cross-reactivity at the level of TCR usage, we performed ex vivo analyses of *TRB* gene expression in both WT and dually reactive WT and Leu268Met KK10-specific $CD8^+$ T cell populations (Figure 2). $CD8^+$ T cell populations specific for the WT epitope were characterized by the turnover of recurrent clonotypes, several of which used the *TRBV4-3* gene as described previously (Iglesias et al., 2011). In contrast, the WT and Leu268Met KK10-specific $CD8^+$ T cell populations comprised entirely distinct clonotypes, suggesting de novo mobilization from the naive pool. The high-avidity WT and Leu268Met KK10-specific $CD8^+$ T cells observed in patients PrInf A and PrInf B showed particular enrichments for TRBV6-5 TRBJ1-1 clonotypes. Furthermore, TRBV6-5 TRBJ1-1 clonotypes were detected in both WT and Leu268Met KK10-specific $CD8^+$ T cell populations in two untreated HLA-B*2705$^+$ patients during the chronic phase of HIV infection (ChInf D and E; Figure S1A). The CDR3β sequence differed by a maximum of three amino acids between these TCRs (Figure 1D), indicating that a TRBV6-5 TRBJ1-1 motif (CASRXGXGXTEAF) can underpin WT and Leu268Met cross-reactivity. Of note, a similar CDR3β sequence was recently detected in an HIV-1-infected patient with elite control of viral replication (Chen et al., 2012). Molecular analysis of *TRA* gene expression revealed that the TRBV6-5 TRBJ1-1 clonotypes were accompanied by TRAV14 TRAJ21 transcripts in the respective $CD8^+$ T cell populations from PrInf

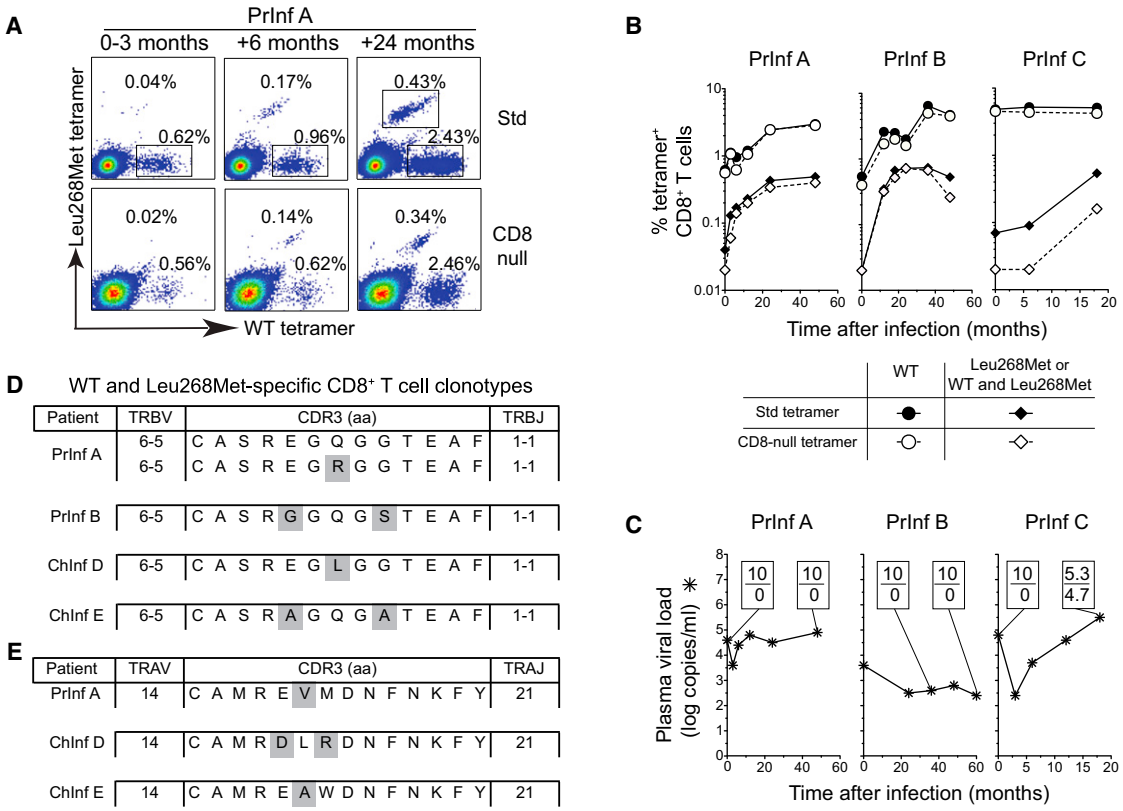

Figure 1. Ex Vivo Analysis of WT and Leu268Met KK10-Specific CD8+ T Cells

(A) Simultaneous WT and Leu268Met HLA-B*2705-KK10 tetramer staining of PBMCs from one HIV-1-infected patient (PrInf A) during and after primary infection. CD8+ T cells were stained with standard (Std) tetramers (top) and CD8-null tetramers (bottom); the latter selectively identify high-avidity cells. The percentages and flow cytometric sorting gates for WT versus Leu268Met or WT and Leu268Met KK10-specific tetramer+CD8+ T cell populations are shown.

(B) Kinetics of WT versus Leu268Met or WT and Leu268Met KK10-specific CD8+ T cell expansions in three patients (PrInf A, B, and C) from primary HIV-1 infection onward. Standard and CD8-null tetramer+CD8+ T cells are shown.

(C) Plasma viral load measurements in three patients (PrInf A, B, and C) from primary HIV-1 infection onward. The Leu268/Met268 ratio within the KK10 epitope is shown at two time points based on viral sequencing from plasma or cell-associated DNA.

(D) CDR3β amino acid sequence of TRBV6-5 TRBJ1-1 clonotypes within WT and Leu268Met KK10-specific CD8+ T cell populations from four HIV-1-infected patients: PrInf A and B (24 and 18 months after primary infection, respectively) and ChInf D and E (chronic infection).

(E) CDR3α amino acid sequence of TRAV14 TRAJ21 transcripts within WT and Leu268Met KK10-specific CD8+ T cell populations from three HIV-1-infected patients: PrInf A (24 months after primary infection) and ChInf D and E (chronic infection).

See also Table S1.

A and ChInf D (Figures 1E and S1B). Moreover, a subdominant TRAV14 TRAJ21 sequence was detected in the Leu268Met KK10-specific CD8+ T cell population in ChInf E. These data support a preferential pairing of TRBV6-5 TRBJ1-1 and TRAV14 TRAJ21 chains in KK10-specific CD8+ T cell clonotypes.

TRBV6-5 TRBJ1-1 Clonotypes Control WT and Leu268Met Viruses Effectively

To evaluate the functional impact of WT and Leu268Met cross-reactivity in more detail, we generated a CD8+ T cell clone (C12C) bearing a TRBV6-5 TRBJ1-1 TRAV14 TRAJ21 TCR (Figure 3A). The functional properties of C12C were evaluated in parallel with two other clones, one with high avidity specifically for the WT KK10 epitope (E2C) and one with low avidity for the same Ag (H8B); the latter clone was included to illustrate poor CD8+ T cell efficacy in our assays (Iglesias et al., 2011). Both WT and Leu268Met HLA-B*2705-KK10 tetramers costained C12C, in contrast to E2C and H8B. Moreover, C12C stained with the corresponding CD8-null tetramers, indicating high levels of avidity for both the WT and Leu268Met epitopes (Figure 3B). This highly avid dual recognition was reflected functionally in cytolytic Cr^{51} release assays, with C12C demonstrating sensitive responses to both forms of the epitope in peptide titrations (Figure 3C). To expand these findings, we measured degranulation (CD107a mobilization) and the intracellular production of IFN-γ, TNF-α, IL-2, and MIP-1β by these clones in response to primary HLA-B*2705+ CD4+ T cells infected with HIV_{NL4-3} viruses expressing either the WT or Leu268Met forms of the KK10 epitope (Figure 3D). In addition, we assessed the elimination of HIV-infected primary HLA-B*2705+ CD4+ target cells in vitro (Figure 3E). In line with the previous results, C12C displayed a robust polyfunctional profile in the presence of either WT or Leu268Met viruses and efficiently suppressed the replication of both HIV strains in primary CD4+ T cells. These features have all been

Patient PrInf A

0-3 months

WT KK10

TRBV	CDR3	TRBJ	Freq (%)	Count	
7-8	CASSSSSQEQF	2-1	39.77	35	
7-8	CASSLEPGTSSYNEQF	2-1	26.14	23	
20-1	CSARDINPGLAYEQY	2-1	13.64	12	
6-2/6-3	CASSPDSNNEQF	2-1	6.82	6	
4-3	CASSQGLQGSEQF	2-1	5.68	5	
5-1	CASSFVDSLSNQPQH	1-5	3.41	3	
9	CASSLHRDTEAF	1-1	3.41	3	
7-8	CASSLEPGTNSYNEQF	2-1	1.14	1	

+3 months

WT KK10

TRBV	CDR3	TRBJ	Freq (%)	Count	
28	CASGDRQNSPLH	1-6	58.70	54	
7-8	CASSSSSQEQF	2-1	26.09	24	
6-5	CASRGTSGTIEQF	2-1	3.26	3	
7-9	CASSLDRNEQF	2-1	3.26	3	*
5-1	CASSFVDSLSNQPQH	1-5	2.17	2	
4-3	CASSQGMFDYGYT	1-2	2.17	2	
12-3/12-4	CASSPTSGIEETQY	2-5	2.17	2	
7-9	CASNLDRNEQF	2-1	1.09	1	
7-8	CANSSSSQEQF	2-1	1.09	1	

+6 months

WT KK10

TRBV	CDR3	TRBJ	Freq (%)	Count
5-1	CASSLRGLAFTSSYNEQF	2-1	31.87	29
4-3	CASSQGQFGNEQF	2-1	28.57	26
7-9	CASSHGDYEQY	2-7	20.88	19
12-3/12-4	CASKKSTGGNTDTQY	2-3	12.09	11
9	CASSVDRDTEAF	1-1	4.40	4
5-1	CASSLRGLASTSSYNEQF	2-1	1.10	1
5-1	CASSLRGLAFSYSYNEQF	2-1	1.10	1

+12 months

WT KK10

TRBV	CDR3	TRBJ	Freq (%)	Count
5-1	CASSFVDSLSNQPQH	1-5	25.88	22
28	CASSSRQNTEAF	1-1	14.12	12
28	CASSDRQNTEAF	1-1	12.94	11
27	CASSHRTGELF	2-2	11.76	10
28	CASGDRQNSPLH	1-6	10.59	9
4-3	CASSQGQFGNEQF	2-1	7.06	6
4-3	CASSSGLAGGREQY	2-7	4.71	4
4-3	CASSQGMFDYGYT	1-2	3.53	3
7-8	CASSSSSQEQF	2-1	3.53	3
4-3	CASSQGLLASLEQY	2-7	2.35	2
10-2	CASRRGGLEIEQY	2-7	2.35	2
28	CAGSSRQNTEAF	1-1	1.18	1

+24 months

WT KK10

TRBV	CDR3	TRBJ	Freq (%)	Count	
28	CASGDRQNSPLH	1-6	45.33	34	
4-3	CASSQGQFGNEQF	2-1	14.67	11	
4-3	CASSPGQYSHEQY	2-7	12.00	9	
27	CASSRNNIEAF	1-1	5.33	4	
29-1	CSVPEQF	2-1	5.33	4	
5-1	CASSFVDSLSNQPQH	1-5	2.67	2	
5-5	CASSLRLLLYEQY	2-7	2.67	2	
27	CATSGITGELF	2-2	2.67	2	
5-1	CASSLRGIQTDSYNEQF	2-1	1.33	1	
5-1	CASSLRGIQTDSHNEQF	2-1	1.33	1	
28	CASSPGTGGDYGYT	1-2	1.33	1	
4-3	CGSSPGQYSHEQY	2-7	1.33	1	
4-3	CVSSQGQFGNEQF	2-1	1.33	1	
28	CASSSRQNTEAF	1-1	1.33	1	#
27	CATSGITRELF	2-2	1.33	1	

+24 months

Leu268Met or WT and Leu268Met

TRBV	CDR3	TRBJ	Freq (%)	Count
6-5	CASREGQGGTEAF	1-1	51.52	34
4-3	CASSLGTSSSYEQY	2-7	28.79	19
6-2	CASTLGTKRF	2-1	16.67	11
6-5	CASREGRGGTEAF	1-1	1.52	1
6-2	CARTLGTKRF	2-1	1.52	1

Patient PrInf B

0-3 months

WT KK10

TRBV	CDR3	TRBJ	Freq (%)	Count	
6-1	CASSSQENTEAF	1-1	57.1	20	
28	CASSDRQNSPLHF	1-6	31.4	11	
7-9	CASSLDRNEQF	2-1	5.7	2	*
5-1	CASSLDPPAGVSPLHF	1-6	2.9	1	
28	CASSSRQNTEAF	1-1	2.9	1	#

+18 months

WT KK10

TRBV	CDR3	TRBJ	Freq (%)	Count	
4-3	CASSQGQLNTQYF	2-3	36.8	25	
7-9	CASSLGEQPQHF	1-5	35.3	24	
28	CASSSRQNTEAF	1-1	7.4	5	#
28	CASSTRQNTEAF	1-1	7.4	5	
4-3	CASSQGRRSIEQF	2-1	4.4	3	
27	CASSSRTGELF	2-2	4.4	3	+
4-3	CASSPGVLGNTIYF	1-3	2.9	2	
28	CASSTRQNAEAF	1-1	1.5	1	

+18 months

Leu268Met or WT and Leu268Met

TRBV	CDR3	TRBJ	Freq (%)	Count
6-5	CASRGGQGSTEAF	1-1	100.0	65

Patient PrInf C

0-3 months

WT KK10

TRBV	CDR3	TRBJ	Freq (%)	Count	
7-9	CASSPYSGSYEQY	2-7	16.46	13	
12-5	CASGLGPSGTEAF	1-1	12.66	10	
20-1	CSARTLEGILTTGETQY	2-5	11.39	9	
27	CASSPRTGELF	2-2	10.13	8	
4-3	CASSLGTSAYEQY	2-7	8.86	7	
25-1	CTRAYNQPQH	1-5	6.33	5	
11-2	CASTIPPGTSVSGELF	2-2	5.06	4	
21-1	CASSKCRDKSYEQY	2-7	2.53	2	
4-3	CASGSGLANNEQF	2-1	2.53	2	
25-1	CASSEGNTGELF	2-2	2.53	2	
27	CASSRHTGELF	2-2	2.53	2	
27	CASRPSNTEAF	1-1	2.53	2	
7-9	CASSLDRNEQY	2-7	2.53	2	
20-1	CSARTLEGILTTGEAQY	2-5	1.27	1	
11-2	CASTIPPRTSVSGELF	2-2	1.27	1	
4-3	CASSPGLATDNEQF	2-1	1.27	1	
9	CASSRADLSYEQY	2-7	1.27	1	
6-5	CASSPGAYGNTIY	1-3	1.27	1	
4-3	CASSLGTSANEQF	2-7	1.27	1	
4-3	CASSQGRRSNEQF	2-1	1.27	1	
27	CASSSRTGELF	2-2	1.27	1	+
27	CASSRRTGELF	2-2	1.27	1	
27	CASSQRTGELF	2-2	1.27	1	
7-9	CASSFDSYEQY	2-7	1.27	1	

+6 months

WT KK10

TRBV	CDR3	TRBJ	Freq (%)	Count
7-9	CASSPYSGSYEQY	2-7	8.33	6
7-9	CASSPRSLSYEQY	2-7	8.33	6
4-3	CASSQGTSDYEQY	2-7	8.33	6
27	CASSQRTGELF	2-2	8.33	6
27	CASSGNTGELF	2-2	6.94	5
7-9	CASSFDSYEQY	2-7	5.56	4
20-1	CSARTLEGILTTGETQY	2-5	4.17	3
11-2	CASTIPPGTSVSGELF	2-2	2.78	2
21-1	CASSKCRGKSYEQY	2-7	2.78	2
4-3	CASGSGLANNEQF	2-1	2.78	2
27	CASSYRTGELF	2-2	2.78	2
27	CASSRSTGELF	2-2	2.78	2
7-9	CASSYDRNEQF	2-1	2.78	2
23-1	CASSHLDSPISNQPQH	1-5	1.39	1
7-9	CASSLGQQISGNTMY	1-3	1.39	1
4-1	CASSQDVLAGRREQY	2-7	1.39	1
29-1	CSVEGGTSGSYEQY	2-7	1.39	1
28	CASSLLGGDLYEQY	2-7	1.39	1
4-3	CASSQGTSDLYEQY	2-7	1.39	1
4-3	CASSLGTSDLYEQY	2-7	1.39	1
9	CASSVADLSYEQY	2-7	1.39	1
9	CASSRADLSYEQY	2-7	1.39	1
7-9	CASSPYSGSYEQF	2-7	1.39	1
4-3	CASSQGVAGAEQY	2-7	1.39	1
4-3	CASSPGTSAYEQY	2-7	1.39	1
4-3	CASSPGLSGNTIY	1-3	1.39	1
28	CASSSLDTGELF	2-2	1.39	1
28	CASSPGDGQPQH	1-5	1.39	1
27	CASSGTLEGGYT	1-2	1.39	1
25-1	CASSEGNTGELF	2-2	1.39	1
7-7	CASSFGQGYEQF	2-1	1.39	1
27	CASSRRTGELF	2-2	1.39	1
27	CASSRHTGELF	2-2	1.39	1
27	CASSGTTGELF	2-2	1.39	1
20-1	CSARTSDFEQF	2-1	1.39	1
7-9	CASTYDRDEQY	2-7	1.39	1
7-9	CASSLDRGDQY	1-5	1.39	1

+18 months

WT KK10

TRBV	CDR3	TRBJ	Freq (%)	Count
27	CASSYRTGELF	2-2	30.00	21
20-1	CSARTLEGILTTGETQY	2-5	12.86	9
9	CASSRADLSYEQY	2-7	10.00	7
4-3	CASSQGLAGREQY	2-7	7.14	5
24-1	CATSDVNGAYEQY	2-7	5.71	4
4-3	CASGSGLANNEQF	2-1	5.71	4
5-1	CASSAESTRLTDTQY	2-3	4.29	3
4-3	CASSQGTSDLYEQY	2-7	4.29	3
7-9	CASSLDRNEQY	2-7	4.29	3
23-1	CASSHLDSPISNQPQH	1-5	2.86	2
4-3	CASSQGTSDYEQY	2-7	2.86	2
4-3	CASSLGQRSTEAF	1-1	2.86	2
7-8	CASSSYRGGGTEAF	1-1	1.43	1
9	CASSRADDSYEQY	2-7	1.43	1
4-3	CASSQGTSDYGQY	2-7	1.43	1
27	CASSYGTGELF	2-2	1.43	1
7-9	CASSYDRNEQF	2-1	1.43	1

+18 months

Leu268Met or WT and Leu268Met

TRBV	CDR3	TRBJ	Freq (%)	Count
20-1	CSARGGSVFYEQY	2-7	48.86	43
20-1	CSARGGERFYEQY	2-7	15.91	14
9	CASSASTSDYSYEQY	2-7	12.50	11
25-1	CASSDLTGTAYNEQF	2-1	11.36	10
20-1	CSDRGGSVFYEQY	2-7	2.27	2
20-1	CSARGGEGFYEQY	2-7	2.27	2
20-1	CSARGGAVFYEQY	2-7	2.27	2
25-1	CASSDLTGTVYNEQF	2-1	1.14	1
20-1	CSAWGGSVFYEQY	2-7	1.14	1
20-1	CSARGRERFYEQY	2-7	1.14	1
4-3	CASSPGVADTQY	2-3	1.14	1

(legend on next page)

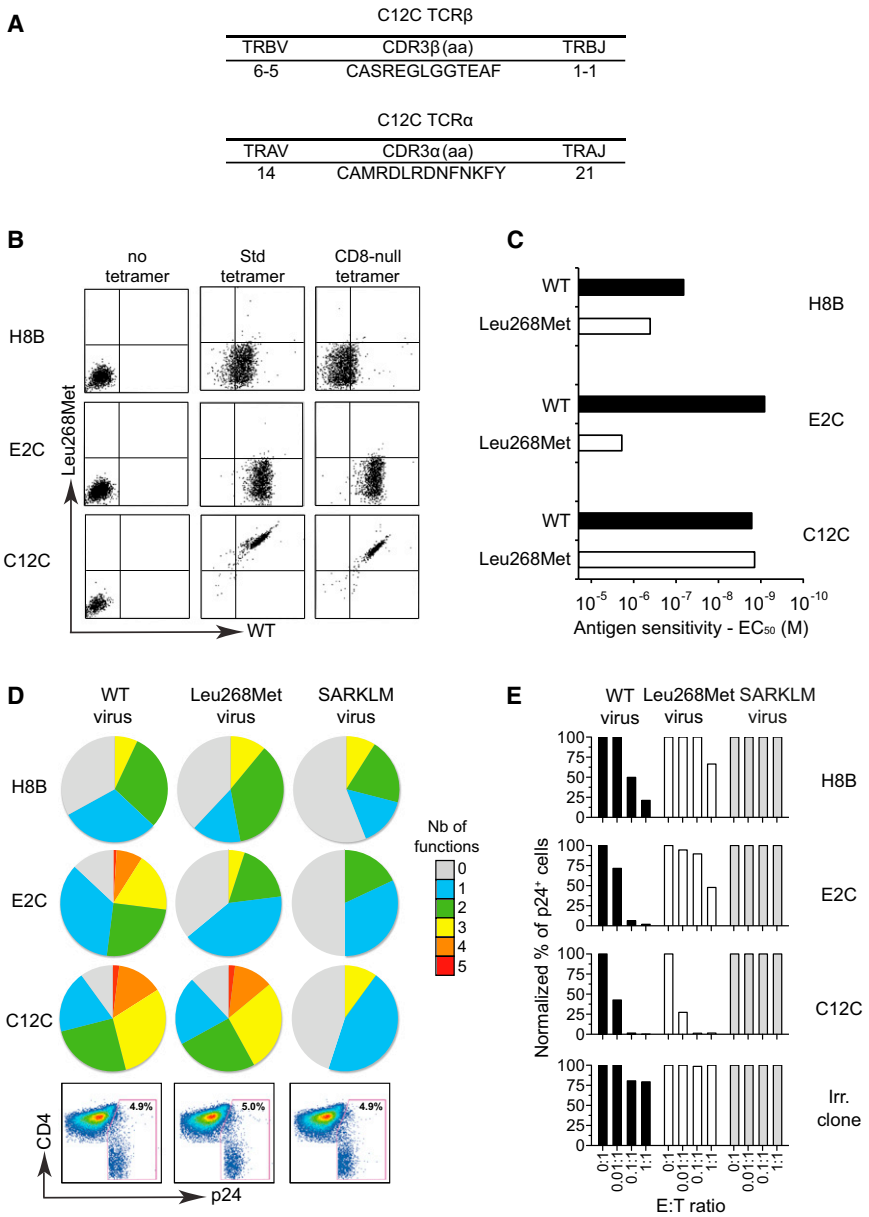

Figure 3. Functional Characterization of the CD8+ T Cell Clone C12C

(A) TCRβ and TCRα amino acid sequences of the C12C clone. This clone was derived from patient ChInf D (Figure S1).

(B) Comparative stainings of three KK10-specific CD8+ T cell clones (H8B, E2C, and C12C) with WT or Leu268Met HLA-B*2705-KK10 tetramers (standard or CD8 null). A pretitrated concentration of each tetramer (0.1 μg/ml) was used to highlight interclonal avidity differences.

(C) Antigen sensitivities (i.e., EC_{50} values in Cr^{51} release assays) of the KK10-specific CD8+ T cell clones H8B, E2C, and C12C.

(D) Polyfunctional profiles of H8B, E2C, and C12C after incubation for 6 hr with primary HLA-B*2705+CD4+ T cells infected with HIV_{NL4-3} viruses expressing either WT, Leu268Met, or the compound Ser173Ala+Arg264Lys+Leu268Met (SARKLM) mutation (CD8:CD4 ratio 10:1). The pie charts depict the background-adjusted polyfunctional profile of the CD8+ T cell clones. For simplicity, responses are grouped according to the number of functions elicited upon antigen encounter; individual segments represent the proportions of cells within each total clonal population that exhibited the number of functions indicated. The following functions were assessed: CD107a, IFN-γ, TNF-α, IL-2, and MIP-1β. In the bottom panel, representative stainings of primary CD4+ T cells at day 3 postinfection with WT, Leu268Met, or SARKLM HIV_{NL4-3} viruses are shown to demonstrate that infection rates (intracellular p24 expression) were equivalent in these experiments.

(E) Suppression of HIV replication in primary HLA-B*2705+CD4+ T cells infected with WT (black bars), Leu268Met (white bars), or SARKLM (gray bars) HIV_{NL4-3} viruses by H8B, E2C, and C12C at different E:T ratios. An irrelevant clone (Irr.) with specificity for an epitope derived from cytomegalovirus is shown as a negative control. The percentage of p24+CD4+ T cells was measured by flow cytometry at day 3 postinfection.

Representative data from three independent experiments are shown.

linked with CD8+ T cell efficacy against HIV in vivo (Appay et al., 2008).

Next, we assessed the impact of C12C on viral selection in vitro. For this purpose, we cocultured target cells infected with both "primary" and "emerging" viruses (e.g., WT and Leu268Met HIV_{NL4-3} strains) together with CD8+ T cell clones, then sequenced the residual viral population (Figure S2). Ratios of WT versus mutant virus were determined according to relative peak height on the sequencing electrogram; this approach was adapted to detect frequencies as low as 10% of the total viral population. Although the suppressive capacity of E2C was evident in this assay (Figure 4A), the presence of this clone resulted in selection of the Leu268Met mutant over the WT virus (Figure 4C), consistent with the inability of E2C to recognize the Leu268Met epitope. In contrast, H8B did not select for the Leu268Met mutant because of its low avidity and poor HIV-suppressive capacity (Figures 4A and 4C). Importantly, C12C suppressed HIV replication efficiently in this assay without selecting for the Leu268Met mutant. These results support our previous observations in vivo that CD8+ T cells with high levels

Figure 2. Clonotype Usage in KK10-Specific CD8+ T Cell Populations from Primary HIV-1 Infection Onward

TRBV and TRBJ usage, CDR3β amino acid sequence, and clonotype frequency are shown for WT and Leu268Met or dually reactive KK10-specific tetramer+CD8+ T cell populations isolated directly ex vivo from three patients (PrInf A, B, and C) during and after primary HIV-1 infection. Representative flow cytometric sorting gates are shown in Figure 1A. Recurrent clonotypes across time points within patients are color coded. Symbols denote public clonotypes within this data set. See also Figure S1.

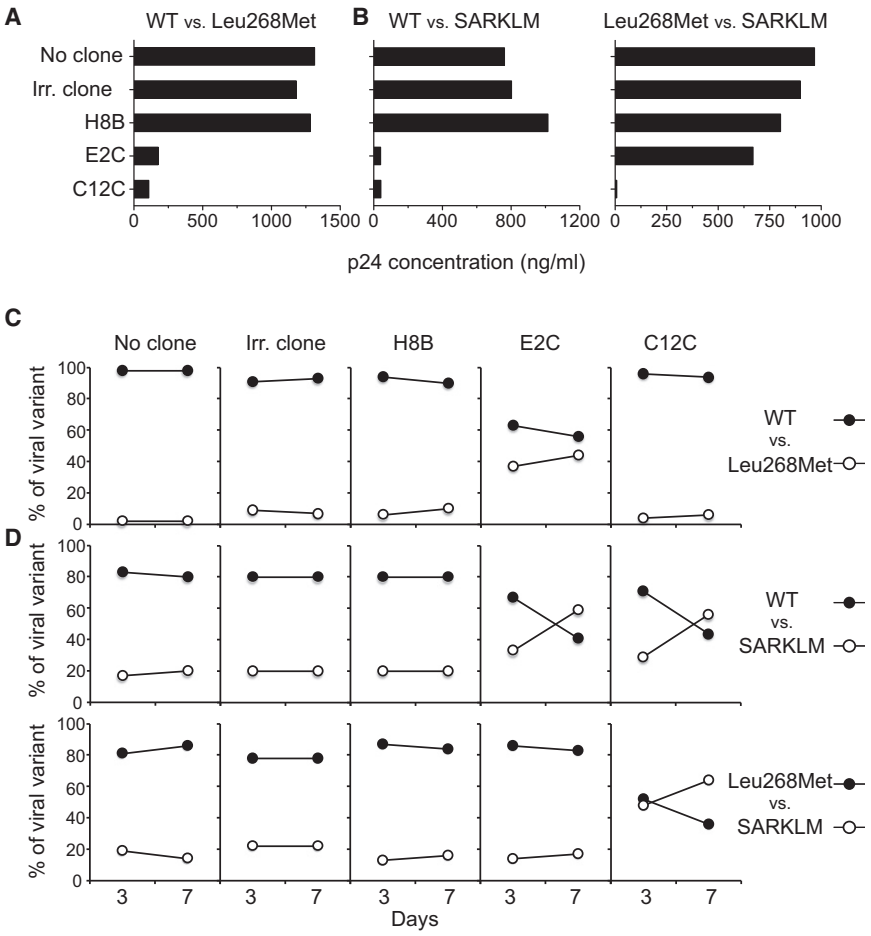

Figure 4. Impact of Distinct CD8+ T Cell Recognition Properties on Viral Selection In Vitro

(A and B) p24 concentrations at day 7 postinfection of 721.221-CD4-B*2705 cells with WT and Leu268Met (A), WT and SARKLM, or Leu268Met and SARKLM (B) viruses in the presence of the indicated CD8+ T cell clones.

(C and D) In vitro selection of viral mutants by KK10-specific CD8+ T cell clones. Percentages of WT and Leu268Met (C), WT and SARKLM, or Leu268Met and SARKLM (D) viruses were determined at day 3 and day 7 postinfection of 721.221-CD4-B*2705 cells cocultured in the presence of the indicated CD8+ T cell clones.

Representative data from two independent experiments are shown. See also Figure S2.

of sensitivity for the WT KK10 epitope in isolation can drive the emergence of early Leu268Met mutants (Iglesias et al., 2011). Collectively, these data indicate that the generation of CD8+ T cells bearing TCRs with dual reactivity can enable the immune system to counter the emergence of Leu268Met mutants.

HLA-B*2705 Recognition by a TRBV6-5 TRBJ1-1 Motif-Bearing TCR

To determine how TRBV6-5 TRBJ1-1 motif-bearing TCRs cross-recognize both the WT and Leu268Met epitopes, we expressed, refolded, and purified the C12C TCR. Surface plasmon resonance experiments showed that the C12C TCR bound both WT and Leu268Met forms of HLA-B*2705-KK10 with equivalent affinities (Kd ~1–5 μM) (Figure S3). This value falls at the high end of the affinity range previously determined for TCR interactions with MHC-I-peptide complexes (Bridgeman et al., 2012) and concurs with the observed tetramer binding and functional properties (Figure 3). Next, we determined the high-resolution crystal structures of the binary WT and Leu268Met HLA-B*2705-KK10 complexes and the corresponding ternary complexes with the C12C TCR (Table 1).

The binary structures showed that the KK10 epitope bound to HLA-B*2705 in a bulged and constrained conformation (Theodossis et al., 2010), with the flexible central part of the peptide protruding from the Ag-binding cleft (Figure 5A). The residues at P2, P3, P8, and P10 were buried in the Ag-binding cleft, whereas the residues at P1, P4–P7, and P9 were solvent exposed. The structure of the Leu268Met HLA-B*2705-KK10 epitope was virtually identical to that of the WT complex, with a root mean square deviation (rmsd) of 0.06 Å and 0.15 Å for the Ag-binding cleft and the peptide, respectively (data not shown). Moreover, the Leu268Met mutation did not affect HLA-B*2705-KK10 complex stability (Tm WT = 63.5°C ± 0.5°C, Tm Leu268Met = 64.0°C ± 1.0°C).

The C12C TCR docked at an angle of 57° across the WT HLA-B*2705-KK10 Ag-binding cleft (Figures 5B and 5C) and adopted a typical binding mode, with the Vα and Vβ domains positioned over the α2 and α1 helices, respectively (Burrows et al., 2010). Located toward the C-terminal end of the HLA-B*2705-KK10 Ag-binding cleft, the C12C TCR formed a total of 124 van der Waals (vdw) interactions and 16 hydrogen (H) bonds with a total buried surface area (BSA) at the interface of ~1,860 Å^2 (Table S2), comprising contributions of 58% and 42% from the Vα and Vβ domains, respectively. All six CDR loops of the C12C TCR contributed to the interaction with WT HLA-B*2705-KK10 (Figure 5C), albeit to varying degrees, with the predominant contacts being made via the CDR2α, CDR3α, and CDR3β loops (19.7%, 24.6%, and 19.8% of the BSA, respectively). Notably, the center of mass of the C12C TCR was shifted toward the α1 helix (77% of the HLA-B*2705 BSA), such that limited contacts were formed with the α2 helix (23% of the HLA-B*2705 BSA). Ligation-induced structural changes are described in Supplemental Information online (Figure S4).

The CDR2α loop was the only region of the C12C TCR that contacted the α2 helix of HLA-B*2705. Further, only two residues (Glu154 and Gln155) of the α2 helix of HLA-B*2705 were contacted by the C12C TCR, thereby representing the smallest contribution by the α2 helix seen in any TCR-MHC-I-peptide structure to date. In contrast, all six CDR loops of the C12C TCR contacted the α1 helix (Table S2). Arg62 was surrounded

Table 1. Data Collection and Refinement Statistics

Data Collection Statistics	C12C-HLA-B*2705^{KK10}	C12C-HLA-B*2705^{L268M}	HLA-B*2705^{KK10}	HLA-B*2705^{L268M}
Space group	$P2_1$	$P2_1$	$P2_12_12_1$	$P2_12_12_1$
Cell dimensions (Å, °)	56.68, 70.32, 107.77; β = 98.77	57.41, 71.31, 109.57; β = 98.80	51.21, 82.33, 109.24	51.27, 82.35, 109.60
Resolution (Å)	2.40 (2.53–2.40)	1.90 (2.00–1.90)	1.60 (1.69–1.60)	1.60 (1.69–1.60)
Total number of observations	243,277 (34,786)	255,452 (37,384)	438,464 (63,793)	409,890 (34,899)
Number of unique observations	32,993 (4,791)	68,882 (10,026)	61,797 (8,892)	55,998 (5,045)
Multiplicity	7.4 (7.3)	3.7 (3.7)	7.1 (7.2)	7.3 (6.9)
Data completeness (%)	100 (100)	99.8 (99.9)	100 (100)	90.5 (57.5)
I/σI	4.5 (1.8)	4.4 (1.6)	7.1 (2.8)	18.3 (4.8)
R_{pim} (%)[a]	5.9 (16.3)	7.0 (27.4)	6.9 (23.6)	2.6 (13.9)
Refinement Statistics				
Nonhydrogen Atoms				
Protein	6792	6884	3269	3277
Water	337	486	585	458
R_{factor} (%)[b]	17.8	18.6	19.7	19.1
R_{free} (%)[b]	25.7	24.5	23.7	22.7
Rms Deviation from Ideality				
Bond lengths (Å)	0.008	0.006	0.006	0.006
Bond angles (°)	1.128	1.022	0.987	1.038
Ramachandran Plot (%)				
Favored and allowed region	99.3	99.6	99.4	99.4
Generously allowed region	0.3	0.4	0.3	0.3
Disallowed region	0.4	0.0	0.3	0.3

Data collection and refinement statistics for the crystal structures of the binary WT and Leu268Met HLA-B*2705-KK10 complexes, as well as the corresponding ternary complexes with the C12C TCR, are indicated. Values in parentheses are for the highest-resolution shell.

[a] R_{pim} = S_h [1(N−1)]$^{1\ 2}$ Si|*Ii*(h) − <I(h)> |ShSi *Ii* (h), where *I* is the observed intensity and <I> is the average intensity of multiple observations from symmetry-related reflections.

[b] R_{factor} = ShkI ||Fo|−|Fc|| S_{hkl} |Fo| for all data except approximately 5%, which were used for R_{free} calculation.

by the CDR1α and CDR2α loops (Figure S5A), whereas the CDR3α loop contacted a more extensive region of the α1 helix (residues 62 to 69). The TCRβ chain contacted a focused region of the α1 helix (positions 72, 76, 79, and 83; Figure S5B). The interactions between the germline-encoded CDR1β and CDR2β loops were quite limited with respect to HLA-B*2705 binding (14.3% and 7.3% of the BSA, respectively), thereby suggesting that the biased *TRBV* gene usage was attributable to indirect mechanisms (Figure S6; Stadinski et al., 2011).

Viral Determinant Recognition by a TRBV6-5 TRBJ1-1 Motif-Bearing TCR

The WT KK10 peptide bulged centrally from the Ag-binding cleft and was contacted by the CDR1α, CDR2α, CDR3α, and CDR3β loops. Unlike the binary WT HLA-B*2705-KK10 structure, the entire region of the peptide was clearly resolved in the ternary complex, indicating that the conformation of the flexible peptide determinant was stabilized and altered by TCR ligation, as observed in other systems (Archbold et al., 2009; Tynan et al., 2007). The C12C TCR pivoted on the P6-Leu residue, and additionally contacted residues P1, P4–P5, P7, and P9, thereby ensuring broad coverage of the viral determinant. The CDR1α and CDR2α loops were positioned over the N-terminal region of the peptide contacting P1, P4, and P6, whereas the CDR3α loop was centrally located contacting P4 and P6, and the CDR3β loop was situated more toward the C-terminal end of the viral peptide contacting P6–P7 and P9 (Figure 5D). The P1-Lys residue was H-bonded to Gln30α, whereas the backbone of the CDR1α loop and Tyr59α from the CDR2α loop packed against the N-terminal "slope" of the peptide. The CDR3β loop was the only region of the TCRβ chain that interacted with the peptide, forming two H-bonds with P7-Gly and P9-Asn and a series of vdw interactions. The majority of these interactions involved Gly109β, Gly111β, and Thr113β, thereby providing structural explanations for both the CDR3β motif and preferential *TRBJ1-1* gene usage (Table S2). Importantly, P6-Leu was sequestered fully by the C12C TCR. The P6-Leu side chain protruded into a central, mostly hydrophobic, pocket that was enveloped by all three CDRα loops and the CDR3β loop and surrounded by a region of the CDR1α main chain, Phe113α, Tyr55α, Arg107α, Gly111β, and Thr113β. Thus, P6-Leu represented the central focal point of the C12C TCR.

The crystal structures of Leu268Met HLA-B*2705-KK10 in isolation and in complex with the C12C TCR showed how the P6-Leu-Met mutation was readily accommodated (Figure 5E). The density of the central region of the Leu268Met peptide was poorly defined in the binary structure, suggesting that the epitope was intrinsically flexible regardless of the amino acid at P6. The C12C TCR docked onto Leu268Met HLA-B*2705-KK10 in essentially an identical manner to that of the cognate

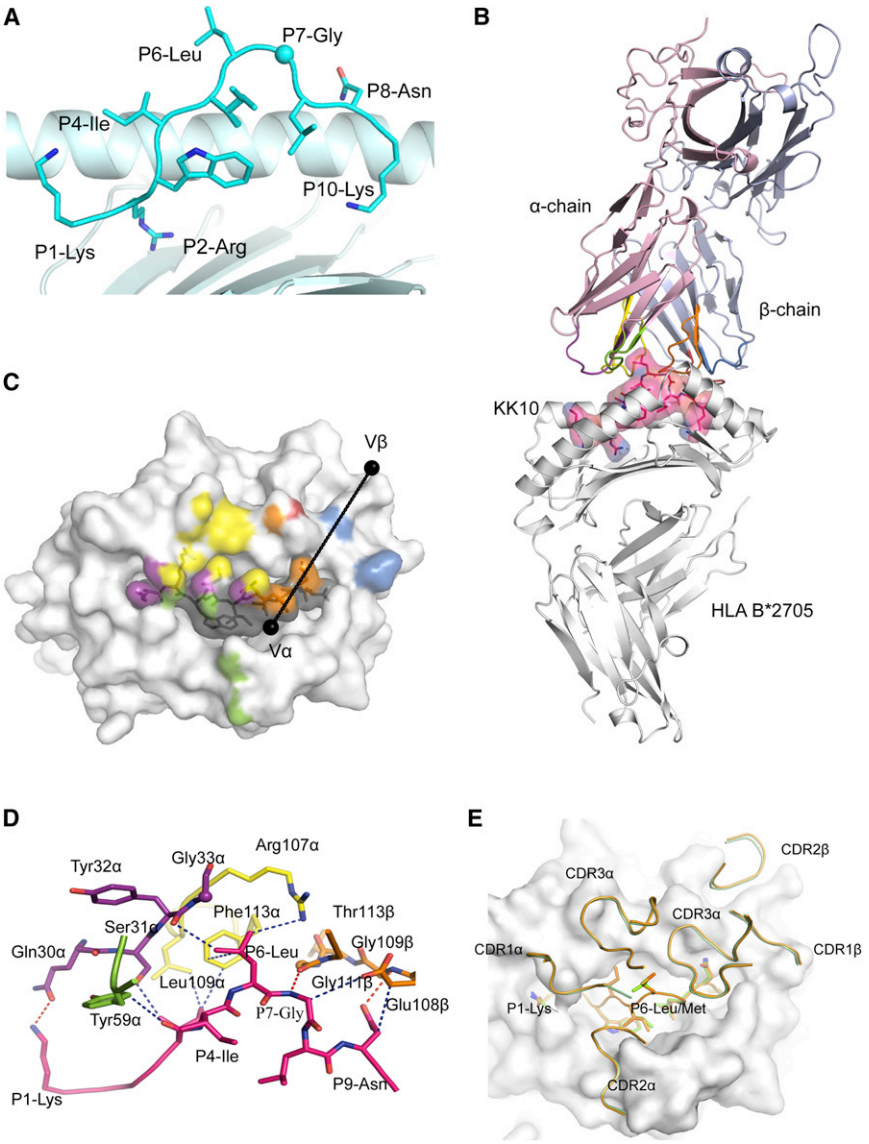

Figure 5. Structure of the C12C TCR in Complex with HLA-B*2705-KK10

(A) Cartoon representation of HLA-B*2705 with KK10 in stick representation. The sphere represents the Cα atom of P7-Gly.

(B) Cartoon representation of the C12C TCR in complex with HLA B*2705-KK10. The α chain of the C12C TCR is colored in pale pink, with the β chain in pale blue. The CDR1, 2, and 3 loops are colored in purple, green, and yellow for TCRα and blue, red, and orange for TCRβ, respectively. The HLA-B*2705 molecule is colored in white and the KK10 epitope is represented in pink stick and surface format.

(C) Footprint of the C12C TCR on the HLA-B*2705-KK10 surface, colored by CDR loop contact as in (B). The black spheres represent the center of mass for the Vα and Vβ domains of the C12C TCR.

(D) Interaction between the KK10 epitope (pink stick) and the C12C TCR loops. The spheres represent the Cα atoms of the glycine residues. The blue dashed lines represent vdw interactions and the red dashed lines represent hydrogen bonds.

(E) Superposition of the C12C TCR in complex with WT and Leu268Met HLA-B*2705-KK10. The peptides are represented in stick format and the CDR loops are shown in cartoon.

See also Figures S3–S6.

WT interaction (rmsd 0.39 Å), revealing that the mutation did not cause a significant repositioning of the C12C TCR (Figure 5E). Instead, P6-Met was located in the same pocket as P6-Leu and formed very similar interactions. Thus, the C12C TCR was perfectly adapted to cope with the P6-Leu-Met substitution, explaining the ability of the corresponding CD8+ T cell clone to cross-recognize both WT and Leu268Met KK10 epitopes and control the emergence of escape mutants.

TRBV6-5 TRBJ1-1 Motif-Bearing TCRs Are Not Readily Generated by Somatic Recombination

Each of the observed TRBV6-5 TRBJ1-1 clonotypes was encoded by only one nucleotide sequence. Analysis of these nucleotide sequences showed that the core of the CASRXGXGXTEAF motif was not predominantly germline encoded (Figure 6A). The two conserved glycines at CDR3β positions 5 and 7 could be completely attributed to the germline genes in only one of the five TRBV6-5 TRBJ1-1 clonotypes. For the other four clonotypes, only one of the two conserved glycines was completely germline encoded, and therefore nucleotide additions were necessary to generate amino acids in direct contact with the WT or Leu268Met peptide (Table S2). In contrast, multiple nucleotide sequences with predominant germline encoding of the associated motif have been observed both within and across individuals for TRBV4-3 TRBJ1-3 clonotypes, which are commonly mobilized and recognize only the WT form of the KK10 epitope with high avidity (Iglesias et al., 2011). Moreover, the TRBV6-5 TRBJ1-1 clonotypes required significantly higher numbers of nucleotide additions compared to the observed TRBV4-3 TRBJ1-3 clonotypes (Figure 6B). These observations suggested that production efficiency for the observed TRBV6-5 TRBJ1-1 clonotypes was relatively low, at least compared to the observed TRBV4-3 TRBJ1-3 TCRs. Thus, although the generation of KK10-specific CD8+ T cells bearing WT and Leu268Met cross-reactive TRBV6-5 TRBJ1-1 TCRs is an effective strategy to combat the appearance of Leu268Met variants, it may be challenging for the immune system to achieve this adaptation.

Eventual Viral Escape from Cross-Reactive WT and Leu268Met KK10-Specific CD8+ T Cells

Faced with TCR repertoire adaptation to viral variants, HIV has developed further means to escape KK10-specific CD8+ T cell recognition, namely the Arg264* mutation. Arg264Lys is the most frequently detected change, although Arg264Thr,

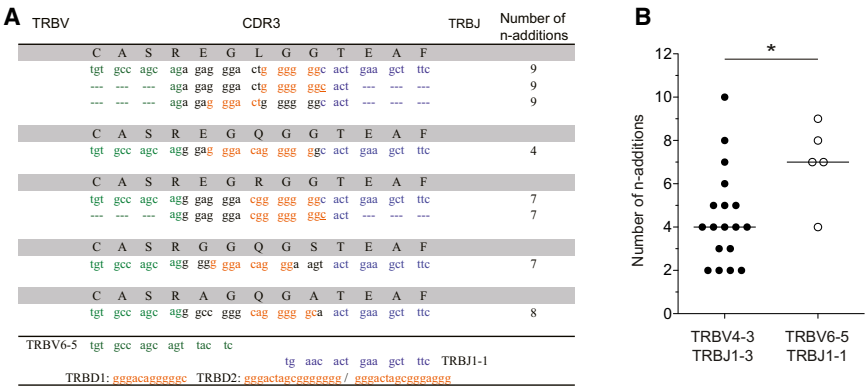

Figure 6. Genetic Coding of KK10-Specific TRBV6-5 TRBJ1-1 Clonotypes

(A) Shown are the observed nucleotide sequences coding for the TRBV6-5 TRBJ1-1 clonotypes described in this study, together with the contributions from the *TRBV* (green), *TRBD* (orange), and *TRBJ* (blue) genes that would require the minimum number of nucleotide additions (black). Potential P-additions are underlined. The multiple lines per nucleotide sequence display the multiple potential recombination events, i.e., different gene contributions and nucleotide additions, that could produce the observed nucleotide sequences with the minimum number of nucleotide additions.

(B) Comparative analysis of the minimal number of nucleotide additions required to generate the observed nucleotide sequences coding for TRBV6-5 TRBJ1-1 clonotypes versus TRBV4-3 TRBJ1-3 clonotypes. The TRBV4-3 TRBJ1-3 clonotypes considered in this analysis were those observed in this and previous studies (Iglesias et al., 2011). Statistical analysis was conducted the Mann-Whitney U-test. *$p < 0.05$.

Arg264Gln, and Arg264Gly substitutions have also been observed (Ammaranond et al., 2005; Betts et al., 2005; Feeney et al., 2004; Goulder et al., 2001; Kelleher et al., 2001; Pillay et al., 2005). The Arg264* mutation occurs at position 2 of the KK10 epitope, which acts as an anchor for HLA-B*27. Accordingly, the observed mutations at this position negatively affect epitope presentation via dramatic reductions in MHC-I-peptide binding affinity, which lead to decreased complex stability on the cell surface and impaired peptide loading during endogenous Ag processing (Ammaranond et al., 2005; Goulder et al., 1997, 2001). However, this mutation also impacts p24 structure and function; consequently, the Ser173Ala compensatory mutation is necessary to restore viral fitness (Schneidewind et al., 2007, 2008). The necessity for two discrete and simultaneous mutations represents a major constraint for the virus and has been proposed as an explanation for the late emergence of Arg264Lys mutants. Nonetheless, the eventual appearance of the Arg264Lys mutation abrogates the efficacy of KK10-specific CD8+ T cells. None of the tested clones, including C12C, were able to suppress replication of a virus displaying the Ser173Ala, Arg264Lys, and Leu268Met mutations (SARKLM) (Figure 3E) or display polyfunctional profiles in the presence of primary HLA-B*2705+ CD4+ cells infected with SARKLM HIV_{NL4-3} (Figure 3D). Furthermore, although both C12C and E2C could drive the selection of the SARKLM mutant against WT virus in vitro, only the WT and Leu268Met cross-reactive clone C12C selected the SARKLM mutant against Leu268Met virus (Figures 4B and 4D). These data are consistent with the notion that SARKLM represents the ultimate escape virus and suggest that immune adaptation to Leu268Met, the early clonotype-specific escape mutant, drives the loss of KK10 binding to eliminate the possibility of further recognition by CD8+ T cells.

DISCUSSION

Viral escape from CD8+ T cell recognition is a hallmark of HIV-1 infection. The first escape variants can replace the original founder virus sequence within days and, as a consequence of ongoing immune pressure, sequential mutations follow (McMichael et al., 2010). Our data highlight the complex balance between viral evolution and immune adaptation focused on a single immunodominant epitope. In the context of HLA-B*2705, the early emergence of Leu268Met mutants is driven by high-avidity CD8+ T cell clonotypes specific for the WT KK10 epitope (Iglesias et al., 2011). The Leu268Met substitution diminishes TCR recognition by these clonotypes, without cost to viral fitness. For HIV-1, this represents a rapid and effortless adaptation to host immunity. New KK10-specific CD8+ T cell clonotypes endowed with WT and Leu268Met recognition capacity can then be recruited from the available repertoire. Indeed, previous studies have also observed changes in the KK10-specific CD8+ T cell repertoire associated with the emergence of Leu268Met variants (Lichterfeld et al., 2007). This alternate clonotypic repertoire is readily able to control HIV-1 replication, as the appearance of the Leu268Met variant does not entail concomitant increases in plasma viremia (Ammaranond et al., 2011; Feeney et al., 2004; Goulder et al., 1997; Kelleher et al., 2001). Nonetheless, this clonotypic restructuring is probably not a trivial undertaking for an immune system already fundamentally compromised by the virus itself, in particular with respect to the loss of memory CD4+ T cells and reduced naive T cell production (Appay and Sauce, 2008; Douek et al., 2009). In addition, WT and Leu268Met cross-reactive clonotypes can be relatively complex to generate. This feature may help to explain the diverse outcomes of HIV-1 infection across HLA-B*2705+ cohorts, despite the overall protection associated with carriage of this allele and the almost universal immunodominance of the KK10 epitope (Goulder and Watkins, 2008). Eventually, though, the highly effective WT and Leu268Met KK10-specific CD8+ T cell response drives the selection of new variants, in particular the Arg264Lys mutation. This new viral variant is more complex to produce because it requires the compensatory Ser173Ala mutation. However, because of the reduction in HLA-B*2705-KK10 peptide binding and presentation, this compound mutation renders the KK10-specific CD8+ T cell response obsolete and therefore represents the ultimate viral adaptation in this system. Uncontrolled HIV-1 replication and disease progression ensue (Almeida et al., 2007; Ammaranond et al., 2011; Feeney et al., 2004; Goulder et al., 1997; Kelleher et al., 2001).

The present work illuminates the mechanism that underpins the control of HIV-1 replication in HLA-B*2705+ individuals,

highlighting the importance of viral variant recognition by KK10-specific CD8+ T cell clonotypes (Chen et al., 2012). It seems likely that the dual specificity TRBV6-5 TRBJ1-1 clonotypes were selected from the available repertoire in response to the emergence of Leu268Met variants. Remarkably, the absence of detectable viral mutants in patients PrInf A and B suggests that such clonotypes may have been elicited by very low-frequency Leu268Met variants, which were subsequently suppressed effectively to the extent that they remained below the limit of detection with conventional subcloning and sequencing approaches. The functional properties of C12C were consistent with this possibility. In addition, a recent study has demonstrated the feasibility of this scenario in another system (Henn et al., 2012). Other clonotypes that recognize Leu268Met less sensitively, as observed in PrInf C, may well require higher frequencies of the variant to be mobilized and will suppress HIV-1 replication less effectively. The early prevalence of the Leu268Met variant in cell-associated DNA from PrInf C and the progressive loss of viral control observed in this patient are compatible with these speculations. Accordingly, the kinetics of the continuous competition between HIV-1 and CD8+ T cell-mediated adaptive immunity are probably critical determinants of viral control and pathogenesis.

Collectively, our findings suggest that the clonotypic nature of the responding CD8+ T cell repertoire and the subtle selection of TCRs conferring high-avidity recognition of both the WT and variant epitopes underpin viremic control and limit the emergence of escape mutations. Analysis of the C12C TCR in complex with HLA-B*2705-KK10 elucidated the molecular basis for effective dual recognition of the WT and Leu268Met epitopes by TRBV6-5 TRBJ1-1 motif-bearing TCRs. Of note, the CDR1β and CDR2β loop interactions were suboptimal with respect to HLA-B*2705 binding, suggesting that biased *TRBV6-5* gene usage may reflect preferred *TRBJ1-1* or *TRAV14* gene pairing. In keeping with this possibility, key residues involved in HLA-B*2705-KK10 binding were encoded only by the *TRAV14* gene. This is consistent with a recent study highlighting the influence of Vα pairing on Vβ recognition of the MHC-peptide complex (Stadinski et al., 2011). These considerations also align well with the observation that *TRAV14* gene usage has been associated with high-avidity WT KK10-specific CD8+ T cell clonotypes (Iglesias et al., 2011).

Other mutations at different positions within the KK10 epitope (e.g., 4, 5, 7, or 9) have been reported and might affect TCR recognition (Almeida et al., 2007; Ammaranond et al., 2011; Feeney et al., 2004; Goulder et al., 1997; Kelleher et al., 2001; van Bockel et al., 2011). These mutations are not associated with enhanced viral replication, suggesting that the capacity of the KK10-specific CD8+ T cell response to recruit cross-reactive clonotypes from the available repertoire is not limited to the Leu268Met variant. Indeed, the TRBV6-5 TRBJ1-1 clonotypes described herein probably represent an array of clonally distributed CD8+ T cells that fulfill the same protective role against HIV. This notion is supported by the observation of various dominant cross-reactive KK10-specific CD8+ T cell clonotypes in HLA-B*2705+ long-term nonprogressors or elite controllers (van Bockel et al., 2011; Chen et al., 2012). Such adaptation within the CD8+ T cell response probably impacts the durability of immune control and biological outcome. More generally, immune adaptation to TCR-accessible mutations may become limiting only in the case of highly restricted epitope-specific repertoires (Price et al., 2004). However, in the case of mutations that adversely impact MHC-I-peptide binding or Ag processing (Goulder and Watkins, 2004), or even lead to epitope deletion from the viral genome altogether (Price et al., 1997), the plasticity of the CD8+ T cell response becomes irrelevant. These considerations explain why the majority of described escape mutations in HIV-1 infection operate to minimize epitope presentation.

The present study provides unprecedented insights into the molecular arms race between HIV and CD8+ T cell immunity within a single epitope specificity. Although the enormity of such reciprocal adaptation across all potential epitopes is staggering, the data reported here illuminate the precarious nature of the incessant battle between host and virus that underlies the apparent equilibrium established during the chronic phase of HIV-1 infection.

EXPERIMENTAL PROCEDURES

Patients

Samples were obtained from asymptomatic HIV-1-infected HLA-B*2705+ patients enrolled in the French ANRS PRIMO cohorts. Antiretroviral therapy was initiated upon evidence of disease progression (i.e., persistent uncontrolled viral replication or CD4+ T cell counts < 500 cells/mm^3), occurring 6 years postinfection for PrInf A and B and 1.5 years postinfection for PrInf C. The study was approved by the Institutional Review Board and Local Ethics Committee of the Hôpital Pitié-Salpêtrière, Paris. Peripheral blood mononuclear cells (PBMCs) were separated from citrate anticoagulated blood and cryo-preserved for subsequent studies. Plasma and cell-associated HIV-1 *gag* sequencing was performed as described previously (Akahoshi et al., 2012).

Viruses and CD8+ T Cell Clones

HIV_{NL4-3} was modified to express one or more mutations in p24 Gag (Ser173Ala, Arg264Lys, and/or Leu268Met) via the GeneTailor site-directed mutagenesis system (Invitrogen) and oligonucleotide primers as described previously (Schneidewind et al., 2007). Viral stocks were generated by transfection of HEK293T cells with 30 μg of plasmid DNA. Supernatants were harvested 48 hr after transfection and frozen aliquots were stored at −80°C. The concentration of p24 Ag in viral stocks was measured by enzyme-linked immunosorbent assay (HIV-1 p24 Ag ELISA kit; ZeptoMetrix). HIV-specific CD8+ T cell clones were generated and maintained as described previously (Almeida et al., 2009). In brief, single HLA-B*2705-KK10 tetramer+CD8+ T cells were sorted by flow cytometry and expanded in microtiter plates by periodic stimulation in the presence of mixed irradiated allogeneic PBMCs, phytohemagglutinin (PHA; 1 μg/ml), and recombinant human IL-2 (rhIL-2; 150 IU/ml) in RPMI 1640 medium supplemented with 5% human AB serum, antibiotics, and L-glutamine.

Clonotype Analysis

Molecular analysis of *TRB* and *TRA* gene expression in KK10-specific tetramer+CD8+ T cell populations isolated directly ex vivo by flow cytometry was conducted via a template-switch anchored RT-PCR as described previously (Quigley et al., 2011). A similar approach was used to characterize *TRB* and *TRA* gene expression in KK10-specific CD8+ T cell clones. In all cases, TCR nomenclature was directly translated from the IMGT database by web-based alignment of molecular TRB or TRA transcripts (IMGT, The ImMunoGeneTics information system, http://www.imgt.org). The germline alignments for the TRBV6-5 TRBJ1-1 clonotypes were determined to allow for potential P-additions from the *TRBD* genes.

Functional Characterization of CD8+ T Cell Clones

Antigen sensitivity was assessed by measuring the peptide concentration required to induce half-maximal responses (EC_{50}) in cytolytic Cr^{51} release

assays with HLA-B*2705+ EBV-transformed B cell targets as described previously (Almeida et al., 2007, 2009). For functional profiling, CD8+ T cell clones were incubated for 1 hr at 37°C in the presence of αCD107a mAb and HLA-B*2705+CD4+ T cells infected 3 days earlier with titrated levels of WT or mutated HIV_{NL4-3} virus; monensin (2.5 μg/ml; Sigma-Aldrich) and brefeldin A (5 μg/ml; Sigma-Aldrich) were added for a further 5 hr. Staining for intracellular markers and data analysis were performed as described previously (Almeida et al., 2009). For HIV suppression assays, primary HLA-B*2705+ CD4+ T cells were purified from PBMCs by positive magnetic bead selection (Miltenyi Biotec), stimulated for 2 days with PHA (1 μg/ml), and cultured with 100 U/ml rhIL-2. Seven days later, 10^5 cells/well were infected with titrated levels of viruses by spinoculation (Iglesias et al., 2011) and mixed with CD8+ T cell clones at different CD8+/CD4+ ratios. Cells were harvested at day 3 postinfection, then stained for both CD4 and intracellular p24 to evaluate the elimination of HIV-infected targets. The protocol for competitive viral selection assays is provided in Supplemental Information online. Directly conjugated mAbs were purchased as follows: from BD Biosciences, αCD4-APCCy7, αCD107a-Cy5PE, αIL-2-APC, αIFNγ-Alexa700, and αTNFα-PECy7; from Caltag Laboratories, αCD8-Alexa405; from R&D Systems, αMIP-1β-FITC; and from Beckman Coulter, αp24-PE. The viability dye ViViD (Life Technologies) was used to eliminate dead cells from flow cytometric analyses.

Protein Production and Crystallography

Soluble recombinant proteins for structural and binding studies were produced as described previously with minor modifications (Gras et al., 2009; Iglesias et al., 2011; Price et al., 2005). Crystals of the C12C TCR in complex with WT and Leu268Met HLA-B*2705-KK10 were grown by the hanging-drop, vapor-diffusion method at 20°C with a protein reservoir drop ratio of 1:1 and a concentration of 5 mg/ml in 10 mM Tris (pH 8), 150 mM NaCl. Crystals grew in 24% PEG 3350 and 0.3 M Na_2SO_4. Crystals of the WT and Leu268-Met HLA-B*2705-KK10 complexes were grown by the same technique in a mother liquor containing 16% PEG 8000 and 0.1 M MES (pH 7.0). Data collection, processing, structure determination, refinement, and validation were conducted with standard crystallography software. Details are provided in Supplemental Information online.

Statistics

Group medians and distributions were compared by the Mann-Whitney U-test. p values less than 0.05 were considered significant.

ACCESSION NUMBERS

The atomic coordinates and structure factors were deposited in the Protein Data Bank with the following accession codes: 4G8G for the C12C TCR in complex with WT HLA-B*2705-KK10, 4G9F for the C12C TCR in complex with Leu268Met HLA-B*2705-KK10, 4G9D for WT HLA B*2705-KK10, and 4G8I for Leu268Met HLA B*2705-KK10.

SUPPLEMENTAL INFORMATION

Supplemental Information includes Supplemental Experimental Procedures, six figures, and two tables and can be found with this article online at http://dx.doi.org/10.1016/j.immuni.2012.11.021.

ACKNOWLEDGMENTS

We thank all study participants, the French Agence Nationale de la Recherche sur le SIDA (ANRS) Cohorts ALT and PRIMO groups, and the staff at the MX2 beamline (Australian synchrotron). We are grateful to C. Blanc for sorting viable infected cells at the Pitié-Salpêtrière Flow Cytometry Platform. This work was supported by the ANR (project ANR-09-JCJC-0114-01), Sidaction, the French ANRS, the National Institutes of Health via the Intramural Program of the Vaccine Research Center (National Institute of Allergy and Infectious Diseases), the Australian Research Council (ARC), the Australian National Health and Medical Research Council (NHMRC), the UK Biotechnology and Biological Sciences Research Council (grant BB/H001085/1), the Japanese Ministry of Health (grant 18390141), and the Global COE program ("Global Education and Research Center Aiming at the Control of AIDS") of the Japanese Ministry of Education, Science, Sports, and Culture. M.C.I. is supported by a Sidaction Fellowship. V.V. and S.G. are ARC Future Fellows. P.G.W. is an NHMRC CJ Martin Fellow. J.R. is an NHMRC Australia Fellow. D.A.P. is a Wellcome Trust Senior Investigator.

Received: March 24, 2012
Accepted: November 5, 2012
Published: March 21, 2013

REFERENCES

Akahoshi, T., Chikata, T., Tamura, Y., Gatanaga, H., Oka, S., and Takiguchi, M. (2012). Selection and accumulation of an HIV-1 escape mutant by three types of HIV-1-specific cytotoxic T lymphocytes recognizing wild-type and/or escape mutant epitopes. J. Virol. *86*, 1971–1981.

Almeida, J.R., Price, D.A., Papagno, L., Arkoub, Z.A., Sauce, D., Bornstein, E., Asher, T.E., Samri, A., Schnuriger, A., Theodorou, I., et al. (2007). Superior control of HIV-1 replication by CD8+ T cells is reflected by their avidity, polyfunctionality, and clonal turnover. J. Exp. Med. *204*, 2473–2485.

Almeida, J.R., Sauce, D., Price, D.A., Papagno, L., Shin, S.Y., Moris, A., Larsen, M., Pancino, G., Douek, D.C., Autran, B., et al. (2009). Antigen sensitivity is a major determinant of CD8+ T-cell polyfunctionality and HIV-suppressive activity. Blood *113*, 6351–6360.

Altfeld, M., Kalife, E.T., Qi, Y., Streeck, H., Lichterfeld, M., Johnston, M.N., Burgett, N., Swartz, M.E., Yang, A., Alter, G., et al. (2006). HLA alleles associated with delayed progression to AIDS contribute strongly to the initial CD8(+) T cell response against HIV-1. PLoS Med. *3*, e403.

Ammaranond, P., Zaunders, J., Satchell, C., van Bockel, D., Cooper, D.A., and Kelleher, A.D. (2005). A new variant cytotoxic T lymphocyte escape mutation in HLA-B27-positive individuals infected with HIV type 1. AIDS Res. Hum. Retroviruses *21*, 395–397.

Ammaranond, P., van Bockel, D.J., Petoumenos, K., McMurchie, M., Finlayson, R., Middleton, M.G., Davenport, M.P., Venturi, V., Suzuki, K., Gelgor, L., et al. (2011). HIV immune escape at an immunodominant epitope in HLA-B*27-positive individuals predicts viral load outcome. J. Immunol. *186*, 479–488.

Appay, V., and Sauce, D. (2008). Immune activation and inflammation in HIV-1 infection: causes and consequences. J. Pathol. *214*, 231–241.

Appay, V., Douek, D.C., and Price, D.A. (2008). CD8+ T cell efficacy in vaccination and disease. Nat. Med. *14*, 623–628.

Archbold, J.K., Macdonald, W.A., Gras, S., Ely, L.K., Miles, J.J., Bell, M.J., Brennan, R.M., Beddoe, T., Wilce, M.C., Clements, C.S., et al. (2009). Natural micropolymorphism in human leukocyte antigens provides a basis for genetic control of antigen recognition. J. Exp. Med. *206*, 209–219.

Arstila, T.P., Casrouge, A., Baron, V., Even, J., Kanellopoulos, J., and Kourilsky, P. (1999). A direct estimate of the human alphabeta T cell receptor diversity. Science *286*, 958–961.

Berger, C.T., Frahm, N., Price, D.A., Mothe, B., Ghebremichael, M., Hartman, K.L., Henry, L.M., Brenchley, J.M., Ruff, L.E., Venturi, V., et al. (2011). High-functional-avidity cytotoxic T lymphocyte responses to HLA-B-restricted Gag-derived epitopes associated with relative HIV control. J. Virol. *85*, 9334–9345.

Betts, M.R., Exley, B., Price, D.A., Bansal, A., Camacho, Z.T., Teaberry, V., West, S.M., Ambrozak, D.R., Tomaras, G., Roederer, M., et al. (2005). Characterization of functional and phenotypic changes in anti-Gag vaccine-induced T cell responses and their role in protection after HIV-1 infection. Proc. Natl. Acad. Sci. USA *102*, 4512–4517.

Bridgeman, J.S., Sewell, A.K., Miles, J.J., Price, D.A., and Cole, D.K. (2012). Structural and biophysical determinants of αβ T-cell antigen recognition. Immunology *135*, 9–18.

Burrows, S.R., Chen, Z., Archbold, J.K., Tynan, F.E., Beddoe, T., Kjer-Nielsen, L., Miles, J.J., Khanna, R., Moss, D.J., Liu, Y.C., et al. (2010). Hard wiring of T cell receptor specificity for the major histocompatibility complex is underpinned by TCR adaptability. Proc. Natl. Acad. Sci. USA *107*, 10608–10613.

Chen, H., Ndhlovu, Z.M., Liu, D., Porter, L.C., Fang, J.W., Darko, S., Brockman, M.A., Miura, T., Brumme, Z.L., Schneidewind, A., et al. (2012). TCR clonotypes modulate the protective effect of HLA class I molecules in HIV-1 infection. Nat. Immunol. *13*, 691–700.

Davis, M.M., and Bjorkman, P.J. (1988). T-cell antigen receptor genes and T-cell recognition. Nature *334*, 395–402.

Dong, T., Zhang, Y., Xu, K.Y., Yan, H., James, I., Peng, Y., Blais, M.E., Gaudieri, S., Chen, X., Lun, W., et al. (2011). Extensive HLA-driven viral diversity following a narrow-source HIV-1 outbreak in rural China. Blood *118*, 98–106.

Douek, D.C., Roederer, M., and Koup, R.A. (2009). Emerging concepts in the immunopathogenesis of AIDS. Annu. Rev. Med. *60*, 471–484.

Feeney, M.E., Tang, Y., Roosevelt, K.A., Leslie, A.J., McIntosh, K., Karthas, N., Walker, B.D., and Goulder, P.J. (2004). Immune escape precedes breakthrough human immunodeficiency virus type 1 viremia and broadening of the cytotoxic T-lymphocyte response in an HLA-B27-positive long-term-nonprogressing child. J. Virol. *78*, 8927–8930.

Goonetilleke, N., Liu, M.K., Salazar-Gonzalez, J.F., Ferrari, G., Giorgi, E., Ganusov, V.V., Keele, B.F., Learn, G.H., Turnbull, E.L., Salazar, M.G., et al.; CHAVI Clinical Core B. (2009). The first T cell response to transmitted/founder virus contributes to the control of acute viremia in HIV-1 infection. J. Exp. Med. *206*, 1253–1272.

Goulder, P.J., and Watkins, D.I. (2004). HIV and SIV CTL escape: implications for vaccine design. Nat. Rev. Immunol. *4*, 630–640.

Goulder, P.J., and Watkins, D.I. (2008). Impact of MHC class I diversity on immune control of immunodeficiency virus replication. Nat. Rev. Immunol. *8*, 619–630.

Goulder, P.J., Phillips, R.E., Colbert, R.A., McAdam, S., Ogg, G., Nowak, M.A., Giangrande, P., Luzzi, G., Morgan, B., Edwards, A., et al. (1997). Late escape from an immunodominant cytotoxic T-lymphocyte response associated with progression to AIDS. Nat. Med. *3*, 212–217.

Goulder, P.J., Brander, C., Tang, Y., Tremblay, C., Colbert, R.A., Addo, M.M., Rosenberg, E.S., Nguyen, T., Allen, R., Trocha, A., et al. (2001). Evolution and transmission of stable CTL escape mutations in HIV infection. Nature *412*, 334–338.

Gras, S., Burrows, S.R., Kjer-Nielsen, L., Clements, C.S., Liu, Y.C., Sullivan, L.C., Bell, M.J., Brooks, A.G., Purcell, A.W., McCluskey, J., and Rossjohn, J. (2009). The shaping of T cell receptor recognition by self-tolerance. Immunity *30*, 193–203.

Henn, M.R., Boutwell, C.L., Charlebois, P., Lennon, N.J., Power, K.A., Macalalad, A.R., Berlin, A.M., Malboeuf, C.M., Ryan, E.M., Gnerre, S., et al. (2012). Whole genome deep sequencing of HIV-1 reveals the impact of early minor variants upon immune recognition during acute infection. PLoS Pathog. *8*, e1002529.

Iglesias, M.C., Almeida, J.R., Fastenackels, S., van Bockel, D.J., Hashimoto, M., Venturi, V., Gostick, E., Urrutia, A., Wooldridge, L., Clement, M., et al. (2011). Escape from highly effective public CD8+ T-cell clonotypes by HIV. Blood *118*, 2138–2149.

Kaslow, R.A., Carrington, M., Apple, R., Park, L., Muñoz, A., Saah, A.J., Goedert, J.J., Winkler, C., O'Brien, S.J., Rinaldo, C., et al. (1996). Influence of combinations of human major histocompatibility complex genes on the course of HIV-1 infection. Nat. Med. *2*, 405–411.

Kawashima, Y., Pfafferott, K., Frater, J., Matthews, P., Payne, R., Addo, M., Gatanaga, H., Fujiwara, M., Hachiya, A., Koizumi, H., et al. (2009). Adaptation of HIV-1 to human leukocyte antigen class I. Nature *458*, 641–645.

Kelleher, A.D., Long, C., Holmes, E.C., Allen, R.L., Wilson, J., Conlon, C., Workman, C., Shaunak, S., Olson, K., Goulder, P., et al. (2001). Clustered mutations in HIV-1 gag are consistently required for escape from HLA-B27-restricted cytotoxic T lymphocyte responses. J. Exp. Med. *193*, 375–386.

Lichterfeld, M., Kavanagh, D.G., Williams, K.L., Moza, B., Mui, S.K., Miura, T., Sivamurthy, R., Allgaier, R., Pereyra, F., Trocha, A., et al. (2007). A viral CTL escape mutation leading to immunoglobulin-like transcript 4-mediated functional inhibition of myelomonocytic cells. J. Exp. Med. *204*, 2813–2824.

Lieber, M.R. (1991). Site-specific recombination in the immune system. FASEB J. *5*, 2934–2944.

McMichael, A.J., Borrow, P., Tomaras, G.D., Goonetilleke, N., and Haynes, B.F. (2010). The immune response during acute HIV-1 infection: clues for vaccine development. Nat. Rev. Immunol. *10*, 11–23.

Moore, C.B., John, M., James, I.R., Christiansen, F.T., Witt, C.S., and Mallal, S.A. (2002). Evidence of HIV-1 adaptation to HLA-restricted immune responses at a population level. Science *296*, 1439–1443.

Nikolich-Zugich, J., Slifka, M.K., and Messaoudi, I. (2004). The many important facets of T-cell repertoire diversity. Nat. Rev. Immunol. *4*, 123–132.

Pillay, T., Zhang, H.T., Drijfhout, J.W., Robinson, N., Brown, H., Khan, M., Moodley, J., Adhikari, M., Pfafferott, K., Feeney, M.E., et al. (2005). Unique acquisition of cytotoxic T-lymphocyte escape mutants in infant human immunodeficiency virus type 1 infection. J. Virol. *79*, 12100–12105.

Price, D.A., Goulder, P.J., Klenerman, P., Sewell, A.K., Easterbrook, P.J., Troop, M., Bangham, C.R., and Phillips, R.E. (1997). Positive selection of HIV-1 cytotoxic T lymphocyte escape variants during primary infection. Proc. Natl. Acad. Sci. USA *94*, 1890–1895.

Price, D.A., West, S.M., Betts, M.R., Ruff, L.E., Brenchley, J.M., Ambrozak, D.R., Edghill-Smith, Y., Kuroda, M.J., Bogdan, D., Kunstman, K., et al. (2004). T cell receptor recognition motifs govern immune escape patterns in acute SIV infection. Immunity *21*, 793–803.

Price, D.A., Brenchley, J.M., Ruff, L.E., Betts, M.R., Hill, B.J., Roederer, M., Koup, R.A., Migueles, S.A., Gostick, E., Wooldridge, L., et al. (2005). Avidity for antigen shapes clonal dominance in CD8+ T cell populations specific for persistent DNA viruses. J. Exp. Med. *202*, 1349–1361.

Quigley, M.F., Almeida, J.R., Price, D.A., and Douek, D.C. (2011). Unbiased molecular analysis of T cell receptor expression using template-switch anchored RT-PCR. Curr. Protoc. Immunol. *10*, 10.33.

Scherer, A., Frater, J., Oxenius, A., Agudelo, J., Price, D.A., Günthard, H.F., Barnardo, M., Perrin, L., Hirschel, B., Phillips, R.E., and McLean, A.R.; Swiss HIV Cohort Study. (2004). Quantifiable cytotoxic T lymphocyte responses and HLA-related risk of progression to AIDS. Proc. Natl. Acad. Sci. USA *101*, 12266–12270.

Schneidewind, A., Brockman, M.A., Yang, R., Adam, R.I., Li, B., Le Gall, S., Rinaldo, C.R., Craggs, S.L., Allgaier, R.L., Power, K.A., et al. (2007). Escape from the dominant HLA-B27-restricted cytotoxic T-lymphocyte response in Gag is associated with a dramatic reduction in human immunodeficiency virus type 1 replication. J. Virol. *81*, 12382–12393.

Schneidewind, A., Brockman, M.A., Sidney, J., Wang, Y.E., Chen, H., Suscovich, T.J., Li, B., Adam, R.I., Allgaier, R.L., Mothé, B.R., et al. (2008). Structural and functional constraints limit options for cytotoxic T-lymphocyte escape in the immunodominant HLA-B27-restricted epitope in human immunodeficiency virus type 1 capsid. J. Virol. *82*, 5594–5605.

Stadinski, B.D., Trenh, P., Smith, R.L., Bautista, B., Huseby, P.G., Li, G., Stern, L.J., and Huseby, E.S. (2011). A role for differential variable gene pairing in creating T cell receptors specific for unique major histocompatibility ligands. Immunity *35*, 694–704.

Streeck, H., Li, B., Poon, A.F., Schneidewind, A., Gladden, A.D., Power, K.A., Daskalakis, D., Bazner, S., Zuniga, R., Brander, C., et al. (2008). Immune-driven recombination and loss of control after HIV superinfection. J. Exp. Med. *205*, 1789–1796.

Theodossis, A., Guillonneau, C., Welland, A., Ely, L.K., Clements, C.S., Williamson, N.A., Webb, A.I., Wilce, J.A., Mulder, R.J., Dunstone, M.A., et al. (2010). Constraints within major histocompatibility complex class I restricted peptides: presentation and consequences for T-cell recognition. Proc. Natl. Acad. Sci. USA *107*, 5534–5539.

Tynan, F.E., Reid, H.H., Kjer-Nielsen, L., Miles, J.J., Wilce, M.C., Kostenko, L., Borg, N.A., Williamson, N.A., Beddoe, T., Purcell, A.W., et al. (2007). A T cell receptor flattens a bulged antigenic peptide presented by a major histocompatibility complex class I molecule. Nat. Immunol. *8*, 268–276.

van Bockel, D.J., Price, D.A., Munier, M.L., Venturi, V., Asher, T.E., Ladell, K., Greenaway, H.Y., Zaunders, J., Douek, D.C., Cooper, D.A., et al. (2011). Persistent survival of prevalent clonotypes within an immunodominant HIV gag-specific CD8+ T cell response. J. Immunol. *186*, 359–371.